Talanta 79 (2009) 1270–1275

Contents lists available at ScienceDirect

Talanta

journal homepage: www.elsevier.com/locate/talanta

Effect of surface microstructures on the separation efficiency of neurotransmitters on a direct-printed capillary electrophoresis microchip

Yu Lu, Yu-Lin Hu, Xing-Hua Xia*

The Key Laboratory of Analytical Chemistry for Life Science (MOE), School of Chemistry and Chemical Engineering, Nanjing University, Nanjing 210093, China

ARTICLE INFO

Article history:
Received 6 January 2009
Received in revised form 19 May 2009
Accepted 21 May 2009
Available online 28 May 2009

Keywords:
Microchip capillary electrophoresis
Surface
Microstructure
Roughness
Separation efficiency

ABSTRACT

The effect of surface microstructures of microchannels on the separation efficiency in microchip electrophoresis has been studied. In order to understand the influence of the surface microstructures on the microchip electrophoresis performance, a thermostatic system was designed and fabricated for precisely control of the chip temperature since the surrounding temperature causes a significant effect on the separation efficiency. The periodically ordered microstructures (dams) of different sizes were fabricated on the microchannels by a simple printing process using different gray levels of the vector graphic software. And the influence of dam sizes in microchannels on the separation efficiency was evaluated by using the number of theoretical plates (N) and the relative resolution (Rs'). Analyzing the variations of mixing elements caused by the periodically ordered dams in the separate channel and elution time, we found that with small dam size fabricated at low gray level of ca. 30%, the resolution of dopamine and epinephrine increased slightly, while it decreased obviously with larger dam sizes especially fabricated at gray level of 50%.

1. Introduction

The field of microfluidics has made considerable progresses due to the distinctive advantages over conventional analytical methods, such as reduced sample consumption, rapid speed, more environmentally appealing, and potential portability and disposability [1–4]. In the early years, the microfluidic devices were mainly fabricated from silicon and glass using the photolithography and etching techniques [5,6], however, the fabrication processes are costly (ca. $200 for a research chip), time-consuming and condition-limited. For avoiding these disadvantages, polymers have been considered as the promise materials for microfluidic devices [7] since they are low cost (ca. $2 for a research chip), and have attractive mechanical and chemical properties, ease of fabrication and higher flexibility [8]. The reported polymeric fabrication techniques include laser ablation [9], plasma etching [10], imprinting [11], hot embossing [12], injection molding [13], and compression molding [14]. Recently, do Lago et al. [15,16] proposed a very simple and convenient microfabrication process based on direct printing for mass production of microfluidic devices at very low cost (ca. 4 cents for a research chip).

Microchip electrophoresis is a fundamental part of microfluidics, which makes use of the phenomenon of electroosmosis as the driving force for separation and liquid transport. Upon application of electric field, buffer solution in the microchannels usually moves from one end to another due to the electrostatically charged surfaces in contact with polar solvents. This phenomenon is termed as electroosmosis. It produces a flat-flow profile compared to the parabolic-flow profile in the pressure-driven flow, significantly minimizing the dispersion of the sample zone. The separation efficiency depends mainly on the control of electroosmotic flow (EOF) and the interactions between analytes and channel-surface in the microchip electrophoresis [17,18]. Electroosmosis is essentially based on the surface chemistry of microchannels and can be adjusted by a variety of methods via adding buffer additives [19–21], altering buffer pH [22–24] and buffer concentration [25], modifying the inner wall of the microchannels or capillaries with nano-composites [26–28]. These methods change the buffer composition or surface properties and result in a new electroosmotic mobility, which contributes to the changes of separation efficiency or satisfies other purposes. Up to now, many reports have focused on the modification of the surface properties to improve the separation efficiency. However, the effect of surface morphology or surface roughness of the microchannels on separation quality is usually neglected. Culbertson and co-workers [29] compared the separation quality on glass microfluidic devices fabricated with photomasks of different optical resolutions by measuring the dispersion (apparent diffusion) coefficiency of a

Abbreviations: N, the number of theoretical plates; Rs', the relative resolution.

* Corresponding author. Tel.: +86 25 83597436; fax: +86 25 83597436.
E-mail address: xhxia@nju.edu.cn (X.-H. Xia).

0039-9140/$ – see front matter © 2009 Elsevier B.V. All rights reserved.
doi:10.1016/j.talanta.2009.05.038

set of standard compounds. Berg and co-workers [30] examined the difference between microchip electrophoresis performances of powder-blasted and hydrogen fluoride-etched microchannels in glass. And recently, the effect of surface roughness was described by mathematical modeling [31]. Obviously, it is essential to understand the effect of surface structure of microchannels on the separation efficiency.

Temperature is usually varied in microchip electrophoresis due to the application of high separation voltages, which will certainly change the diffusion coefficient of solute, the viscosity of solvent, and the surface properties of the microchannels due to the Joule effect. It is clear that precisely control of the surrounding temperature of microchannels is essential for obtaining reproducible and repeatable results, especially in the study of biochemical systems. Therefore, many researchers have proposed various approaches to control the surrounding temperature of the microchip. Verpoorte and co-workers [32] designed an integrated temperature control system for microfluidic devices which could regulate the local temperature by using the chemical and physical processes. Chen and co-workers [33] suggested the integration of a commercial heat sink for computer central processor unit (CPU) on polydimethylsiloxane (PDMS) microchip electrophoresis system, and the Joule heat and heat dissipation from the high separation voltage could be eliminated efficiently. Jiang and co-workers [34] reported an autonomously triggered on-chip microfluidic cooling device utilizing temperature-responsive hydrogels to recirculate cooler water automatically.

In this paper, the effect of microstructures of microchannels on electrophoretic separation efficiency in microchip electrophoresis has been investigated. The periodically ordered structures (dams) of different sizes were designed using different gray levels of vector graphic software and then transferred onto transparencies by a laser printer. Dopamine and epinephrine were used as model system to study the effect of the dam sizes on the separation efficiency. In order to understand the effect of surface roughness of the microchannels on the separation efficiency, a thermostatic system was designed to precisely control the temperature of the microchip electrophoresis system for avoiding the effect of variation of surrounding temperature. Two main factors influencing the separate efficiency in this system, the changes of the elution time and mixing elements causing perturbation of laminar flow of liquid due to periodic ordered dams on the surface were discussed.

2. Experimental

2.1. Materials and reagents

Transparency film CG3300 (3M, Italy) was used as the base material. The stock solutions of dopamine (Sigma, USA) and epinephrine (Sigma, USA) were prepared by dissolving the reagents in a 1 mM $HClO_4$ aqueous solution to reach the final concentration of 10 mM. Both stock solutions of dopamine and epinephrine were kept at 4 °C. Sample solutions were prepared by diluting the stock solutions with running buffer prior to use. The phosphate buffer (pH 7.4, 10 mM) solution (PBS) served as the running buffer. All reagents were of analytical grade and used without further purification. All aqueous solutions were prepared from deionized water (18 MΩ, PURELAB Classic, PALL, USA). All solutions were passed through a 0.22 μm cellulose acetate filter (Xinya Purification Factory, Shanghai, China) before electrophoresis measurements.

2.2. Microfabrication process

The basic procedure used to fabricate microchips has been described previously in detail [16]. The layouts of cover slip of different gray levels in separation microchannel and the substrate slip with smooth separation microchannel were designed using the standard computer software Adobe Illustrator 10.0 and then was printed out in a 1:1 scale on transparency films by an EPL 5800 Laser Printer (Epson, Japan) with the toner cartridge S050010 at 1200 dots per inch (dpi). As shown in Fig. 1A, after the holes for fluid access were drilled in the cover slip (Fig. 1A (a)) using a paper puncher, the substrate slip (Fig. 1A (b)) and cover slip were laminated using a heat laminator (Fig. 1A (c)). Fig. 1B shows the schematic layout of the designed microchip in the vertical view. The separation channel (a to e, 60 mm) contained an effective separation channel (o to e, 50 mm) in which the length of different gray levels (f to e, 48 mm) was printed. The width of both separation and injection channels was designed to be 150 μm, which was set by the Adobe Illustrator 10.0. Taking advantage of the laser-printing mechanism, periodically ordered dams consist of plenty of micrometer toner particles were transferred onto transparencies by

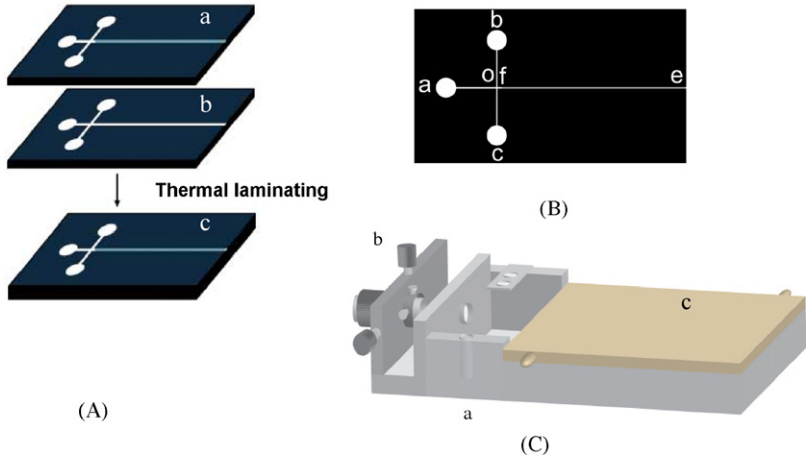

Fig. 1. Schematic layouts of the PET-toner microchip and homemade plexiglass holder. (A) Schematic representation of the fabrication procedure of the PET-toner microchip: (a) cover slips, (b) substrate slip, (c) the substrate slip and cover slip were laminated. (B) The configuration of PET-toner microchip: (a) buffer reservoir, (b) sample reservoir, (c) sample waste reservoir, (e) end-channel detection point. Separation channel with a total length, (a–e) 60 mm; effective length, (o–e) ≈50 mm; length of gray levels ≈48 mm. Injection channel with a total length (b, c) 20 mm. The width of the channels was 150 μm (not to scale). (C) The three-dimensional view of the homemade plexiglass holder integrated with a supporting frame (a) a three-dimensional micromanipulator: *X*-, *Y*-, *Z*-direction adjustor (b) and a thermostatic copper hollow plate (c).

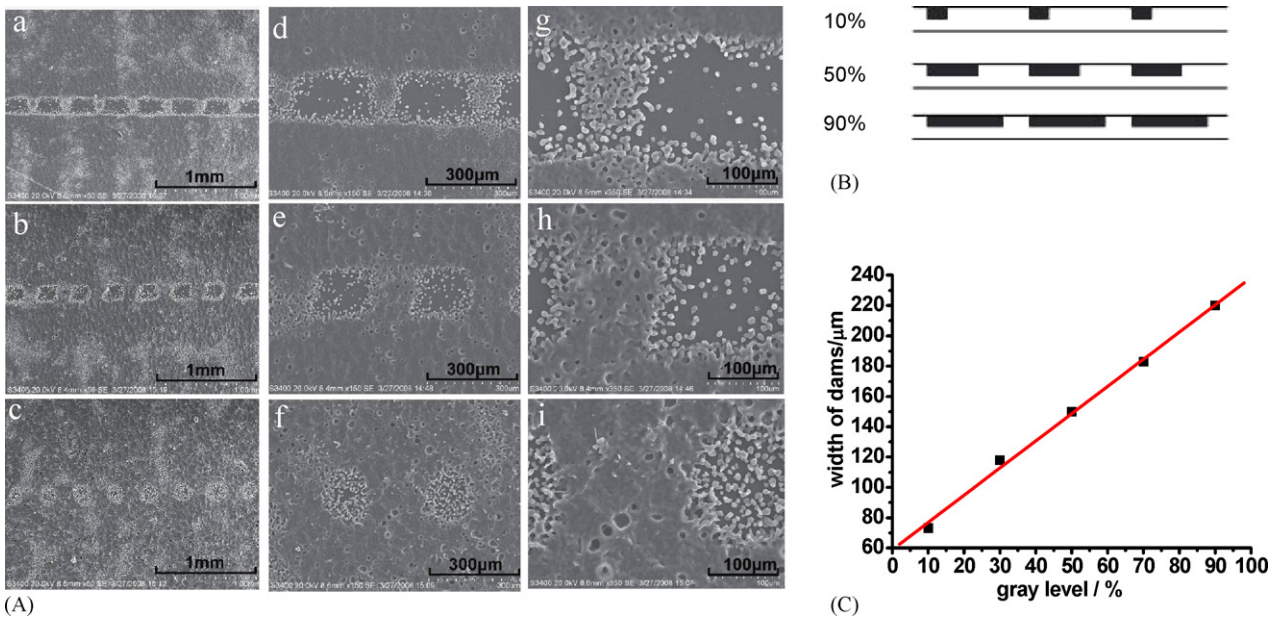

Fig. 2. (A) SEM images of microstructures of the cover slips designed by different gray levels before the lamination with substrate slip. (a–c, d–f, g–i) The top views of microstructures with larger magnification respectively. Gray level: (a, d, g) 10%, (b, e, h) 50%, (c, f, i) 90%. (B) Cross-sectional schematic layout of separation channels. (C) The linear relationship between the width of dams and gray levels.

using different gray levels of vector graphic software [35,36]. Fig. 2A represents the SEM images of the separation channels with periodic dams created by different gray levels. As shown in Fig. 2B, the cross-sectional schematic layout of the separation channels is displayed in detail. The channels had 11 ± 0.5 μm in height in the region of the microchannels without dams and the height of dams is approximately 7 ± 0.5 μm as measured from the SEM images [33]. For the dam prepared using a gray level of 10%, its width in the direction of microchannel was 73 ± 5 μm. As shown in Fig. 2C, it increased with the increase of gray scale linearly and was 118 ± 5 μm, 150 ± 5 μm, 183 ± 5 μm and 220 ± 5 μm respectively at the gray level of 30%, 50%, 70% and 90%. Furthermore, the rectangular region of the channel within the cofines of toner decreased gradually as the increase of gray level and its shape turned into circle at the gray level of 90% due to the increase of the micrometer toner particles in this region gradually.

2.3. Apparatus

A home-made plexiglass holder with thermostatic copper hollow plate was fabricated for fixing the microchip, housing the detector and regulating the temperature of the microchip. As shown in Fig. 1C, the holder is composed of a supporting frame, a reservoir, a 3-D micromanipulator and the constant temperature cabinet. The waste reservoir e (the total system size is 60 mm long, 15 mm wide and 7 mm high) was served as both the cathodic buffer reservoir for the CE system and the electrochemical detection cell. The 3-D micromanipulator (Shanghai Lianyi Instrument Factory of Optical Fiber and Laser, Shanghai, China) was fixed on the plexiglass holder for precisely aligning the working electrode to the end of the microchannels. The thermostatic hollow plate was made up of copper (the total size is 80 mm long, 70 mm wide and 10 mm high) including an inlet and an outlet of fluids through which water with constant temperature (precision within ±0.1 °C) was circulated by utilizing a thermostat (Chengdu Instrument Factory, Chengdu, China). The steadily fixing of the microchips on the thermostatic plate adjacent to the edge of the reservoir was achieved by using silicone grease and double-sided adhesive tap to prevent the microchips from buffer solution permeation.

Alignment of the working electrode to the microchannel end was performed under a microscope (Jiangnan Optical Instrument Factory, Nanjing, China). An Ag/AgCl reference electrode, a platinum wire counter electrode and a ground Pt electrode for CE were also placed in the reservoir along with a homemade carbon disk working electrode [34,37]. Amperometric detection was carried out in a three-electrode configuration with an Electrochemical Workstation CHI 650 (Shanghai Chenhua Instrument Company, Shanghai, China).

3. Experiment procedures

3.1. Electrophoresis

For each new microchip, the channels were washed with deionized water for 2 min. After the deionized water was taken out of the microchannels using a vacuum pump, the microchips were laminated again at 120 °C in the laminator. Then, they were rinsed with buffer solution for several minutes without remaining gas bubbles in the microchannels. Electrophoresis experiments were carried out by a laboratory made voltage power supply with a voltage range from +150 V to +5000 V. The applied voltage could be automatically controlled by a personal computer via an AD/DA converter. The separation current could be real time monitored and the corresponding data could be saved in text files. As shown schematically in Fig. 1B, the voltages were applied to the separation (between a and e) and injection channels (between b and c) respectively for several minutes until the separation and injection currents leveled off. The electrochemical detection reservoir was also restocked with fresh buffer. The buffer reservoirs (a and c) and the sample reservoir (b) were restocked with fresh buffer and fresh sample, respectively. The injection was carried out by applying a high voltage (HV) to the sample reservoir for a given time via the Pt electrodes connected to the HV power supply, with the sample waste reservoir (c) grounded and the other reservoirs floating. Once sample injection was completed, separation voltage was applied to the buffer reservoirs (a) with the detection reservoir (e) grounded and the other reservoirs floating. Electrophoresis separation of the neurotransmitters were carried out for three times by using three same types of microchips for each different dam sizes inside the microchannel.

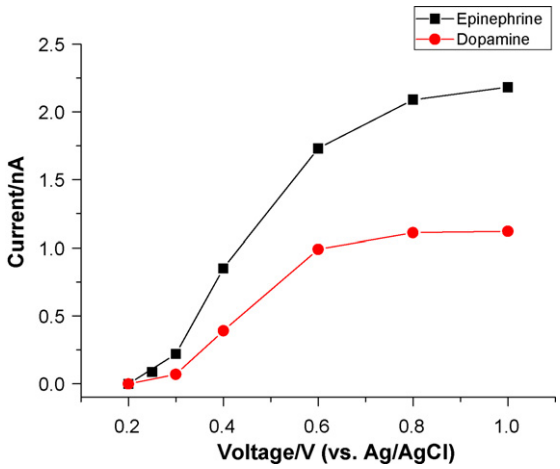

Fig. 3. Hydrodynamic voltammograms of 100 μM dopamine (●) and 100 μM epinephrine (■) on a carbon disk electrode in running buffer. Conditions: separation voltage: 1200 V; sample injection: at 800 V for 15 s; working electrode: A 300 μm-diameter carbon disk electrode; running buffer: phosphate buffer (pH 7.4, 10 mM).

3.2. Constant temperature control

Constant surrounding temperature of the microchips was precisely controlled during each electrophoresis separation experiment. After the steadily fixing of the microchip on the constant temperature cabinet, constant temperature water was circulated by the thermostat through the inlet and an outlet. The required surrounding temperature of the microchip was reached after several minutes as indicated by the separation current leveled off. All the experiments were performed under precisely temperature control.

3.3. Electrode preparation

A 300 μm-diameter carbon disk electrode was made from pencil lead (Staedtler, German), used as the working electrode for detection. Detailed fabrication procedure was described elsewhere [34]. Amperometric detection was carried out in a three-electrode configuration, a carbon working electrode, an Ag/AgCl reference electrode and a platinum wire counter electrode.

3.4. Safety consideration

The high-voltage power supply should be handled with extreme caution to avoid an electric shock. Due to the high conductivity of the copper, contact of the ground Pt electrode for CE and the copper constant temperature cabinet should be avoided.

4. Results and discussion

4.1. Influence of the detection potential

The detection potential plays an important role in the separation and electrochemical detection system. Fig. 3 shows the hydrodynamic voltammograms of dopamine and epinephrine on a 300 μm carbon microelectrode in PBS. The oxidation peak currents for both analytes started at 0.30 V and increased rapidly with the increase of detection potential up to 0.8 V. When the potentials exceeded 1.00 V, the peak currents for both analytes increased slowly. Since too much higher anodic detection potential will result in higher background current, the detection potential in microchip system was set at 1.0 V.

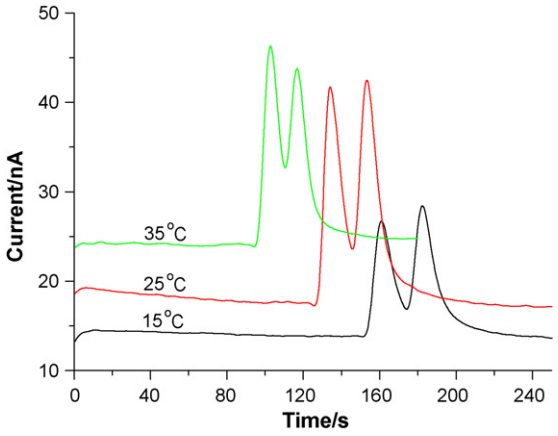

Fig. 4. Influence of surrounding temperature (from 15 °C to 35 °C) on the electropherograms. Other conditions were the same as in Fig. 3.

4.2. Influence of the surrounding temperature

The temperature of microchip electrophoresis is usually generated due to the high separation voltage which affects the separation performance. Its tiny variation can lead to significant change in the elution time during the experiment. Therefore, a thermostatic system was designed in microchip capillary electrophoresis to keep the surrounding temperature of microchips constant and to improve the precision and reproducibility of migration time. During experiments, each separation current can be monitored graphically in real time. As expected, different surrounding temperature results in different leveling-off separation current. Fig. 4 shows the influence of surrounding temperature on the amperometric response and separation efficiency. It clearly showed that with the decrease of temperature from 35 °C to 15 °C, the elution time increased significantly from 102.6 s to 160.9 s and from 116.7 s to 182.3 s for dopamine and epinephrine, respectively. At the same time, the resolution of the analytes was improved obviously. Taking consideration of the obviously poor resolution of the analytes at 35 °C and the long elution time of the analytes at 15 °C, the surrounding temperature was set at 25 °C for the following investigations.

4.3. Effect of the microstructures on the separation efficiency

The interior environment of microchannel is the main factor which affects the electrodynamic behavior including electroosmosis and electrophoresis. The increased wall roughness may affect the fluid flow within the channels and furthermore, the separation efficiency. The surface properties of the interior wall may lead to the variation of electroosmotic flow including its direction and velocity. In addition, the laminar flow of liquid will be perturbed. Thereby, the separation efficiency highly depends on the surface properties of the interior wall of separation microchannels. In order to understand this effect, periodically ordered dams were fabricated on the microchannel using different gray levels of vector graphic software by a laser printer. Such ordered dams can be regard as efficient rough elements in microchannels. Fig. 5 shows the effects of the dam sizes inside the microchannels on the separation efficiency denoted by the number of theoretical plates per meter (N) and relative resolution (Rs'). This two parameters ware calculated as follows:

$$N = 20 \times 5.54 \times \left(\frac{t_{R1}}{W_{h/2}}\right)^2 \quad (1)$$

$$\text{Rs'} = \frac{2(t_{R2} - t_{R1})}{W_{h/2} + W_{h/2}} \quad (2)$$

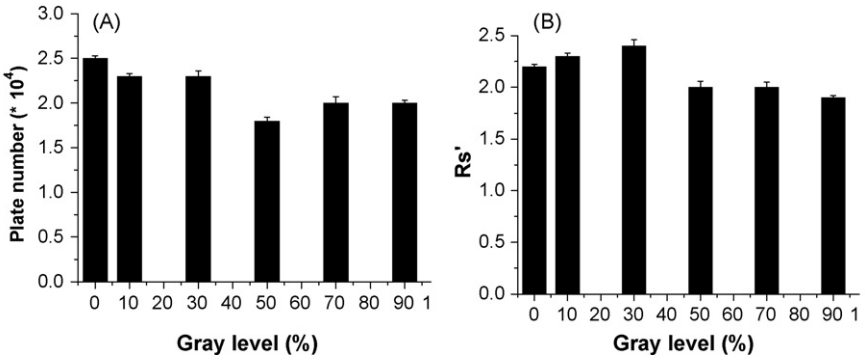

Fig. 5. Effects of the different gray levels inside the microchannels on the number of theoretical plates (A) and relative resolution (B).

where t_{R1}, t_{R2} are the migration time of dopamine and epinephrine, respectively; $W_{h/2(1)}$, $W_{h/2(2)}$ are the peak width at half height of dopamine and epinephrine, respectively. Each parameter was the average of the results obtained in three microchips for each different gray level. The standard deviation of each data was indicated as error bars. As it is shown, the variation of the data is smaller than the difference of each measurement for both the Rs' and N.

As expected, the number of theoretical plates gradually decreased with the increase of dam size in generally (Fig. 5A). With larger dam size created at the gray level of 50%, the plate number was the lowest. With further increase of the dam size, it increased again gradually. On the contrast, the Rs' did not continuously decrease as the dam sizes increased as shown in Fig. 5B, which is not expected. When dam size was smaller than it created at gray level 30%, the Rs' even slightly increased with the increase of dam sizes. With larger dam sizes larger than it created at gray level 50%, the Rs' gradually decreased with the increase of dam size.

Based on these phenomena, it is clear that there are two main factors that determine the behavior of electrophoresis: mixing elements caused by the periodically ordered dams leading to perturbation of laminar flow of liquid and the change of elution time due to the varied properties of the heterogeneous surfaces of the microchannels. As we reported previously [35], high mixing efficiency (lamellae reduction factor of 85%) could be achieved at a distance of 500 μm downstream of the microchannels patterned with mixing elements created with gray levels of 50% to 80%. Although the width of the microchannels and the patterns of the microstructures were not exactly the same as those in ref. [35], we believe that this mixing effect should be considered in the present case. The factor was validated by the result in Fig. 5A. With the enhancement of the mixing efficiency, the plate number should be decreased inch by inch. With large dam size created at the gray level of 50%, the full mixing effect resulted in the lowest plate number. With the further increase of the dam size, the mixing efficiency decreases, resulting in the gradual increase in plate number.

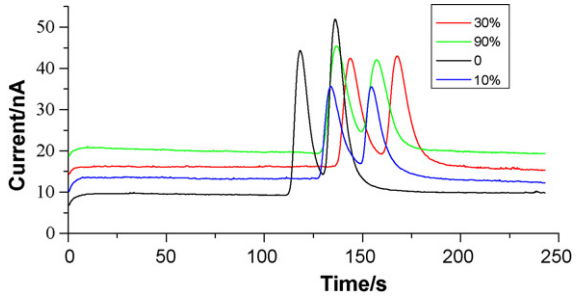

Fig. 6. Influence of the microstructures patterned with different gray level (from 0% to 90%) inside the microchannels on the electropherograms. Other conditions were the same as in Fig. 3.

On the other hand, the resolution of the separation in electrophoresis can be calculated from the following Eq. (3) [38]

$$R = \left(\frac{1}{4\sqrt{2}}\right)(\Delta\mu_{app})\left(\frac{V}{D(\bar{\mu}+\mu_{eo})}\right)^{1/2} \quad (3)$$

where V is the applied separation voltage, D is the diffusion coefficient, μ_{eo} is the electroosmotic mobility, $\bar{\mu}$ represents the average of two analytes' electrophoretic mobilities, and $\Delta\mu_{app}$ represents the distinction of two analytes' electrophoretic mobility. From Eq. (3), we can definitely infer that the separation resolution R has an affinitive relationship with $\bar{\mu}$ and μ_{eo}, namely, the better separation efficiency can be obtained at slower elution mobility. As shown in Fig. 6, the migration time of the analytes and the separation quality gradually increased with the increase of dam size created at gray level lower than 30%, though broadening of the sample bands occurred. This result is in good accordance with the expectation from Eq. (3). However, with larger dam sizes created at the gray level larger than 30%, the migration time of the analytes decreased with the increase of dam size. Understanding of this behavior needs further investigation.

Based on the above analysis, it is clear that the two main factors of elution time and mixing effect of the microchannels patterned with microstructures determine mainly the separation quality. At gray level lower than 50%, the mixing efficiency increases with the dam size [35], resulting in the decrease in the separation quality. At the same time, the elution time of the analytes increases with the dam size as well, resulting in the increase of the separation quality. Therefore, the separation efficiency of the analytes in the microstructures patterned microchannels is determined by the balance of these two factors. With dam size created at the gray level of 30%, the best separation efficiency can be obtained (Fig. 5B). With dam size created at the gray level higher than 50%, the mixing efficiency increases with the increase of dam size; while the elution time decreases with the increase of dam size. Both of these two factors result in the decrease in separation quality.

5. Conclusions

In this work, we have investigated the effect of surface microstructures on the separation efficiency on a direct-printed capillary electrophoresis microchip. The results show that the surface microstructures of the microchannels play an important role in determining the separation efficiency of neurotransmitters besides the effect of surrounding temperature. The reasons for the different performances of the microchannels patterned with dams of different sizes using different gray level are related to two main factors: the mixing elements and the changes of elution time caused by the periodic ordered microstructures in the microchannels. With dam sizes created at gray level lower than 50%, the separation efficiency is determined by the balance of these two factors due to the oppo-

site effects caused by the increase of mixing efficiency and elution time; while with dam size created at the gray level higher than 50%, both the increase of mixing efficiency and decrease of the elution time resulted in the decrease in separation efficiency. Furthermore, the understanding of the effect of microstructures on the separation efficiency on capillary electrophoresis microchip is surely helpful to control the roughness of microchannels during the microfabrication and optimize the separation conditions during microchip capillary electrophoresis.

Acknowledgements

The authors greatly acknowledge the financial support from the National Basic Research Program (2007CB714501), the National Natural Science Foundation of China (20535010, 20775035, 20890020), the Ministry of Education of China (no. 200802840012) and the National Science Fund for Creative Research Groups (20821063).

References

[1] D.R. Reyes, D. Iossifidis, P.A. Auroux, A. Manz, Anal. Chem. 74 (2002) 2623.
[2] P.A. Auroux, D. Iossifidis, D.R. Reyes, A. Manz, Anal. Chem. 74 (2002) 2637.
[3] T. Vilkner, D. Janasek, A. Manz, Anal. Chem. 76 (2004) 3373.
[4] P.S. Dittrich, K. Tachikawa, A. Manz, Anal. Chem. 78 (2006) 3887.
[5] Q.F. Xue, F. Foret, Y.M. Dunayevskiy, P.M. Zavracky, N.E. McGruer, B.L. Karger, Anal. Chem. 69 (1997) 426.
[6] A. Scherer, S.R. Quake, Science 290 (2000) 1536.
[7] H. Becker, C. Gartner, Electrophoresis 21 (2000) 12.
[8] J.C. McDonald, D.C. Duffy, J.R. Anderson, D.T. Chiu, H.K. Wu, O.J.A. Schueller, G.M. Whitesides, Electrophoresis 21 (2000) 27.
[9] M.A. Roberts, J.S. Rossier, P. Bercier, H. Girault, Anal. Chem. 69 (1997) 2035.
[10] J. Rossier, F. Reymond, P.E. Michel, Electrophoresis 23 (2002) 858.
[11] L. Martynova, L.E. Locascio, M. Gaitan, G.W. Kramer, R.G. Christensen, W.A. MacCrehan, Anal. Chem. 69 (1997) 4783.
[12] G.B. Lee, S.H. Chen, G.R. Huang, W.C. Sung, Y.H. Lin, Sens. Actuators B: Chem. 75 (2001) 142.
[13] R.M. McCormick, R.J. Nelson, M.G. Alonso-Amigo, D.J. Benvegnu, H.H. Hooper, Anal. Chem. 69 (1997) 2626.
[14] Y. Liu, D. Ganser, A. Schneider, R. Liu, P. Grodzinski, N. Kroutchinina, Anal. Chem. 73 (2001) 4196.
[15] C.L. Lago, H.D.T. Silva, C.A. Neves, J.G.A. Brito-Neto, J.A.F. Silva, Anal. Chem. 75 (2003) 3853.
[16] C.L. Lago, W.K.T. Coltro, J.A.F. Silva, H.D.T. Silva, E.M.R. Richter, L. Angnes, L.H. Mazo, E. Carrilho, Electrophoresis 25 (2004) 3832.
[17] D. Belder, M. Ludwig, Electrophoresis 24 (2003) 3595.
[18] B.J. Kirby, J.E.F. Hasselbrink, Electrophoresis 25 (2004) 187.
[19] J.W. Jorgenson, K.D. Lukacs, Science 222 (1983) 266.
[20] C. Schwer, E. Kenndler, Anal. Chem. 63 (1991) 1801.
[21] M. Grob, F. Steiner, Electrophoresis 23 (2002) 1853.
[22] W.J. Lambert, D.L. Middleton, Anal. Chem. 62 (1990) 1585.
[23] C. Chaiyasut, Y. Takatsu, S. Kitagawa, T. Tsuda, Electrophoresis 22 (2001) 1267.
[24] H. Yu, F.Y. He, Y. Lu, Y.L. Hu, H.Y. Zhong, X.H. Xia, Talanta 75 (2008) 43.
[25] H.J. Issaq, I.Z. Atamna, G.M. Muschik, G.M. Janini, Chromatographia 32 (1991) 155.
[26] M. Pumera, J. Wang, E. Grushka, R. Polsky, Anal. Chem. 73 (2001) 5625.
[27] G.T. Roman, T. Hlaus, K.J. Bass, T.G. Seelhammer, C.T. Culbertson, Anal. Chem. 77 (2005) 1414.
[28] W. Wang, L. Zhao, J.R. Zhang, X.M. Wang, J.J. Zhu, H.Y. Chen, J. Chromatogr. A 1136 (2006) 111.
[29] A.R. Meyer, A.M. Clark, C.T. Culbertson, Lab Chip 6 (2006) 1355.
[30] Q.S. Pu, R. Luttge, H.J.G.E. Gardeniers, A.V.D. Berg, Electrophoresis 24 (2003) 162.
[31] Y.D. Hu, C. Werner, D.Q. Li, Anal. Chem. 75 (2003) 5747.
[32] R.M. Guijt, A. Dodge, G.W.K. Dedem, N.F. Rooij, E. Verpoorte, Lab Chip 3 (2003) 1.
[33] Y. Zhang, N. Bao, X.D. Yu, J.J. Xu, H.Y. Chen, J. Chromatogr. A 1057 (2004) 247.
[34] A.K. Agarwal, L. Dong, D.J. Beebe, H. Jiang, Lab Chip 7 (2007) 310.
[35] A.L. Liu, F.Y. He, K. Wang, T. Zhou, Y. Lu, X.H. Xia, Lab Chip 5 (2005) 974.
[36] A.L. Liu, F.Y. He, Y.L. Hu, X.H. Xia, Talanta 68 (2006) 1303.
[37] F.Y. He, A.L. Liu, X.H. Xia, Anal. Bioanal. Chem 379 (2004) 1062.
[38] J.W. Jorgenson, K.D. Lukacs, Anal. Chem. 53 (1981) 1298.